

## **Environmental indicator for effective control of COVID-19 spreading**

**Xinbo Lian<sup>1</sup>, Jianping Huang<sup>1,2,\*</sup>, Li Zhang<sup>1</sup>,**

**Chuwei Liu<sup>1</sup>, Xiaoyue Liu<sup>1</sup>, Lina Wang<sup>3</sup>**

<sup>1</sup> Collaborative Innovation Center for Western Ecological Safety, College of Atmospheric Sciences, Lanzhou University, Lanzhou, 730000, China.

<sup>2</sup>CAS Center for Excellence in Tibetan Plateau Earth Sciences , Beijing 100101,China.

<sup>3</sup>Gansu Province Environmental Monitoring Center, Lanzhou, 730000, China.

Corresponding Author :

Dr. Jianping Huang ( [hjp@lzu.edu.cn](mailto:hjp@lzu.edu.cn) )

## Abstract

Recently, a novel coronavirus (COVID-19) has caused viral pneumonia worldwide, spreading to more than 200 countries, posing a major threat to international health. To prevent the spread of COVID-19, in this study, we report that the city lockdown measure was an effective way to reduce the number of new cases, and the nitrogen dioxide (NO<sub>2</sub>) concentration can be adopted as an environmental lockdown indicator. In China, after strict city lockdown, the average NO<sub>2</sub> concentration decreased 55.7% (95% confidence interval (CI): 51.5-59.6%) and the total number of newly confirmed cases decreased significantly. Our results also indicate that the global airborne NO<sub>2</sub> concentration steeply decreased over the vast majority of COVID-19-hit areas based on satellite measurements. We found that the total number of newly confirmed cases reached an inflection point about two weeks after the lockdown. The total number of newly confirmed cases can be reduced by about 50% within 30 days of the lockdown. The stricter lockdown will help newly confirmed cases to decline earlier and more rapidly. Italy, Germany and France are good examples. Our results suggest that NO<sub>2</sub> satellite measurement can help decision makers effectively monitor control regulations to reduce the spread of COVID-19.

## 1 **1. Introduction**

2 Large-scale COVID-19 viral pneumonia through human-to-human transmission poses a  
3 severe and acute public health emergency (Huang et al., 2020a; Li et al., 2020). As the epidemic  
4 worsened, most countries imposed city lockdown and quarantine measures to reduce  
5 transmission to control the epidemic. The Chinese government has gradually implemented a  
6 city-wide quarantine of Wuhan and several surrounding cities as of 23 January, flights and trains  
7 to and from Wuhan have been suspended, and public transport has been halted (Cyranoski et al.,  
8 2020; Wu et al., 2020). The entire northern Italy was quarantined since 9 March 2020, and three  
9 days later the government extended it to the whole country (Paterlini, 2020).The Spanish  
10 government declared a 15-day national emergency, starting on 15 March (Legido-Quigley et al.,  
11 2020). In the United States, on 19 March, California became the first state to order a lockdown  
12 (Baccini et al., 2020). In Germany, since 18 March, 16 states have closed, public gatherings of  
13 more than two people have been banned and most shops except supermarkets and pharmacies  
14 have closed (Dehning et al., 2020). On 23 March, the British government announced a new  
15 nationwide restriction allowing residents to only venture outside when absolutely necessary, e.g.,  
16 to work, buy necessities (Iacobucci, 2020).

17 The worldwide lockdown, which was imposed to stop the spread of the novel coronavirus,  
18 not only caused an economic downturn but also appeared to result in cleaner air in urban areas  
19 usually heavily affected by pollution (Lian et al., 2020; Schiermeier, 2020). The most important  
20 measure of the lockdown policy was the reduction of traffic and control personnel flow, and  
21 traffic pollution is an important factor influencing air quality and public health. Vehicle exhaust  
22 and evaporation emissions are the main emission sources of ozone and secondary particle

23 precursors near the ground in cities and regions (Zhou et al., 2019; Yuan et al., 2013), and the  
24 spatial variation of nitrogen dioxide (NO<sub>2</sub>), fine particulate matter (PM<sub>2.5</sub>) and black carbon (BC)  
25 may also be significant affected by traffic flow density (Clougherty et al., 2013). A study in Los  
26 Angeles showed that nitrogen oxides (NO<sub>x</sub>) were identified as a source of pollution for light  
27 vehicles, with NO<sub>2</sub>, NO<sub>x</sub>, carbon dioxide (CO<sub>2</sub>), BC, and fine particle number (PN<sub>fine</sub>) identified  
28 as diesel exhaust sources (Tessum et al., 2018; Fan et al., 2018). In South Korea, source analysis  
29 studies have shown that there is a high correlation between estimated traffic volume and NO<sub>2</sub>  
30 concentration (Kim et al., 2015). NO<sub>2</sub> levels can be used as a proxy for exposure to  
31 traffic-related composite air pollution and to assess the impact of scenarios designed to reduce  
32 traffic-related emissions (Brnum-Hansen et al., 2018; Johansson et al., 2017).

33 In this report, we study the parameters of environmental indicators for city lockdown. Using  
34 the automatic ground detection data and satellite data to analyze the trend of lockdown and the  
35 total confirmed new cases in major cities in China, and using satellite data to further study the  
36 impact of lockdown on virus transmission in countries mainly severely affected by the epidemic,  
37 in order to help policymakers to formulate effective control measures to reduce the spread of  
38 COVID-19.

39

## 40 **2. Data and measurement**

41 The ground observation daily data were provided by the China National Environmental  
42 Monitoring Centre (<http://www.cnemc.cn/>). The data from January 24, 2020, to February 23,  
43 2020, are selected as the representative data after the lockdown in Hubei, and the data from

44 December 24, 2019, to January 23, 2020, are selected as the representative data before the  
45 lockdown (Fig. 1). The NO<sub>2</sub> ground observation data of China is from 1 January 2020 to 1  
46 March 2020. The average concentration of major cities with severe epidemic diseases was  
47 selected as the representative of NO<sub>2</sub> concentration of China, including Wuhan, Nanchang,  
48 Guangzhou, Hangzhou, Changsha, Beijing, Shanghai, Hefei and Zhengzhou (Fig. 3). All  
49 monitoring instruments of the air quality automatic monitoring system operate automatically 24  
50 h a day. The monitoring items are PM<sub>2.5</sub>, PM<sub>10</sub>, SO<sub>2</sub>, NO<sub>2</sub>, and CO. The automatic monitoring of  
51 PM<sub>2.5</sub> and PM<sub>10</sub> adopts the micro-oscillating balance method and the β-absorption method,  
52 respectively (ambient air quality standards, GB 3095-2012). SO<sub>2</sub> was determined by the  
53 ultraviolet fluorescence method, NO<sub>2</sub> by the chemiluminescence method, CO by the  
54 nondispersion infrared absorption method and gas filter correlation infrared absorption method.

55 This paper adopted the level 3 daily global gridded (0.25°×0.25°) nitrogen dioxide product  
56 (OMNO2d) provided by the Ozone Monitoring Instrument (OMI) onboard the Aura satellite as  
57 the daily NO<sub>2</sub> data, which can be obtained from GES DISC  
58 ([https://disc.gsfc.nasa.gov/datasets/OMNO2d\\_003](https://disc.gsfc.nasa.gov/datasets/OMNO2d_003)). The Aura satellite was launched by NASA  
59 on July 15, 2004, with its overall objective of monitoring the chemistry and dynamics of the  
60 atmosphere from the ground to the mesosphere. The OMI is a nadir-viewing charge-coupled  
61 device (CCD) spectrometer onboard the Aura satellite, whose observation band is  
62 near-UV/visible. We selected the Column Amount NO<sub>2</sub> Trop product to calculate the changes in  
63 the tropospheric NO<sub>2</sub> concentration impacted by the control measures in East Asia, Western  
64 Europe and North America (Fig. 2):

65 
$$VA = \frac{N_2 - N_1}{N_1} \times 100\% \quad (1)$$

66

67 where VA is the relative variation ratio, N1 is the average NO<sub>2</sub> concentration in the  
68 troposphere one month before the lockdown, and N<sub>2</sub> is the average NO<sub>2</sub> concentration in the  
69 troposphere one month after the lockdown.

70 The data from 1 January 2020 to 3 March 2020, were selected to analyze the variation in  
71 NO<sub>2</sub> over time in China (Fig. 3). The NO<sub>2</sub> satellite data of Italy, Germany, France, the United  
72 States, Iran and Switzerland is from the time of the first case in each country to 20 April 2020  
73 (Fig. 4). Due to the satellite orbit, default values occur among the daily data that were  
74 determined via piecewise linear interpolation over time. Border data from the US Centers for  
75 Disease Control and Prevention (CDC)  
76 (<https://www.cdc.gov/epiinfo/support/downloads/shapefiles.html>) were selected to obtain the  
77 borders of each country. To remove the influence of weather factors, a 7-day moving average  
78 was calculated. To compare the relative changes among the different countries, the data for each  
79 country were standardized.

80 The daily total number of new confirmed cases in each country and region was obtained  
81 from the Center for Systems Science and Engineering (CSSE) of Johns Hopkins University  
82 (<https://github.com/CSSEGISandData/COVID-19>). The daily total number of new confirmed  
83 cases in China was retrieved from the Department Earth System Science of the Tsinghua  
84 University shared case database (<https://cloud.tsinghua.edu.cn/d/335fd08c06204bc49202/>).

85

### 86 3. Results analysis

#### 87 3.1. A spatial comparison of pollutants before and after lockdown in Hubei Province.

88 Fig. 1 shows the change in pollutant concentration in Hubei Province one month before and  
89 after the closure of major cities severely affected by the epidemic. Compared with before the  
90 lockdown, NO<sub>2</sub>, sulphur dioxide (SO<sub>2</sub>), particulate matter (PM<sub>10</sub>), carbon monoxide (CO) and  
91 PM<sub>2.5</sub> concentrations all decreased to a certain extent, while NO<sub>2</sub> experienced the most notable  
92 decrease. Since biomass and coal combustion are major SO<sub>2</sub> and CO sources, they exhibit the  
93 lowest rate of improvement (Khalil et al., 1988; Huang et al., 2012). Both the PM<sub>2.5</sub> and PM<sub>10</sub>  
94 concentrations decreased to a certain extent (31.2% and 34.3%, respectively) as a result of the  
95 reduction in fugitive dust, particulate matter and important precursors produced by motor  
96 vehicles and factories (Huang et al., 2019). The monthly average PM<sub>2.5</sub>/PM<sub>10</sub> ratio was 0.81 (95%  
97 confidence interval (CI): 0.76-0.86), so PM<sub>2.5</sub> was the main particle pollutant after lockdown.  
98 Exhaust emissions contributed only moderately to local levels of the PM<sub>2.5</sub> total mass, which  
99 were mostly derived from other sources, such as biomass combustion and the remote  
100 transmission of secondary particles (Chen et al., 2012). Therefore, the impact of strict traffic  
101 control during the lockdown on PM<sub>2.5</sub> is not notable, and the spatial difference is large, so PM<sub>2.5</sub>  
102 is not suitable as a city lockdown indicator.

103 Although the NO<sub>2</sub> emissions per vehicle slightly decreased after the upgrading of the  
104 quality standards of petroleum products, the notable growth of vehicle ownership increased the  
105 proportion of NO<sub>2</sub> traffic source emissions, in addition, after the implementation of emission  
106 standards for coal-fired power plants, multiple technical improvements greatly controlled the  
107 NO<sub>2</sub> emissions from coal-fired sources, which all enhanced the correlation between NO<sub>2</sub> and city

108 lockdown effect (Liu et al., 2020). The effect of city closure on NO<sub>2</sub> was significantly greater  
109 than that on the other pollutants, with an average concentration reduction of approximately 60.3%  
110 (95% CI: 56.8-64.0%), which can be applied as an environmental indicator of the lockdown  
111 effect.

112

### 113 3.2. Changes of airborne NO<sub>2</sub> plummets over COVID-19-hit area after lockdown.

114 In East Asia (Fig. 2a), satellite images show that compared to before the blockade, the total  
115 emissions of NO<sub>2</sub> in eastern China have significantly decreased by approximately 56.6%. In  
116 South Korea, the monthly NO<sub>2</sub> emissions have also been reduced by approximately 18.0 %. The  
117 local government has implemented the most expansive testing programme and has isolated  
118 people infected with the virus without locking down entire cities, and the sharp decrease in NO<sub>2</sub>  
119 may be linked to the reduction in local emissions and pollutant transport from surrounding areas  
120 (Han, 2019; Bauwens et al., 2020). Japan has not imposed widespread lockdown policies, and a  
121 4.8% increase in NO<sub>2</sub> may be linked to emissions from power generation and industrial  
122 processes (Han, 2019). In western Europe (Fig. 2b), the monthly NO<sub>2</sub> concentrations have  
123 decreased sharply in Italy by 47.5%, particularly in the north (82.4%), where the outbreak is the  
124 most severe. This could be due to the reduction in road traffic and the decrease in economic  
125 activities in the industrial heartland as a result of the widespread lockdown policy (Schiermeier,  
126 2020). Other countries such as Germany, Denmark, and Poland also experienced notable  
127 reductions. This is consistent with the results of the European Environment Agency (EEA) (EEA,  
128 2020). However, in certain areas, such as northern and southern Spain, the NO<sub>2</sub> concentration  
129 has risen, possibly because of lax closure measures and increased emissions from coal-fired

130 power plants (Curier et al., 2014). In the United States (Fig. 2c), one month after the lockdown,  
131 the overall decline in NO<sub>2</sub> is relatively small. The worst affected states, such as New York,  
132 Washington and California, still contain areas with increased NO<sub>2</sub> concentrations, and the NO<sub>2</sub>  
133 concentration is increasing significantly in the vast midwestern regions that have not yet been  
134 locked down.

135  
136 3.3. The temporal evolution of the NO<sub>2</sub> concentration and the total number of newly confirmed  
137 cases in China.

138 After the strict city lockdown, the NO<sub>2</sub> concentration in the main virus-affected cities in  
139 China decreased significantly (Fig. 3). Consistent with the satellite data, the ground monitoring  
140 results showed that compared to the conditions before the closure, the monthly average NO<sub>2</sub>  
141 concentration after the lockdown decreased approximately 55.7% (95% CI: 51.5-59.6%). Since  
142 the lockdown, the total number of confirmed new cases reaches an inflection point after  
143 approximately two weeks (the incubation period of the virus is 14 days), and compared to the  
144 period of 1-15 days after the closure, the total number of confirmed new cases in the 16-30 days  
145 after the closure has decreased 73.6% (95% CI: 64.9-81.1%). The most significant improvement  
146 was recorded in Hangzhou, where the NO<sub>2</sub> concentration decreased approximately 68.1%, and  
147 the total number of confirmed new cases declined the most. Likewise, Zhengzhou, Changsha,  
148 Guangzhou, and Nanchang are good examples. Wuhan, the worst virus-affected area in China,  
149 also exhibited a downward trend. The total number of confirmed new cases reached 13,436 on  
150 February 12 due to the inclusion of clinically diagnosed cases (Wei et al., 2020), resulting in a  
151 new delayed peak in the figure.

152 The national emergency response has delayed the spread of the epidemic and greatly limited  
153 its range. The suspension of intra-city public transport, the closure of entertainment venues and  
154 the banning of public gatherings have been linked to a reduction in the incidence of cases.  
155 Studies have shown that before emergency response initiation, the basic case reproduction  
156 number ( $R_0$ ) is 3.15, and after intervention measures were implemented in 95% of all places, the  
157 average  $R_0$  value has dropped to 0.04, the total number of actual cases has decreased 96% (Tian  
158 et al., 2020).

159

160 3.4. The temporal evolution of the  $\text{NO}_2$  concentration and the total number of newly confirmed  
161 cases in the COVID-19-hit areas globally.

162 After the countries severely affected by COVID-19 implemented strict lockdown measures,  
163 satellite data showed a significant decline in  $\text{NO}_2$  emissions, and the total confirmed new cases  
164 decreased after two weeks in most areas (Fig. 4). As a result, the strict lockdown of  
165 COVID-19-hit areas other than those in China is also effective and easy to implement to prevent  
166 the spread of the virus. The lockdown measures might have already prevented tens of thousands  
167 of deaths in Europe (Flaxman et al., 2020). In Italy, where the epidemic is widespread, after the  
168 lockdown the  $\text{NO}_2$  emissions significantly decreased by an average of 36.6%, and the total  
169 confirmed new cases reached an inflection point 12 days later, thus verifying that the spread of  
170 the virus was effectively controlled. Studies have shown that 38,000 deaths have been averted in  
171 this country due to the implemented intervention measures (Flaxman et al., 2020). The  
172 occurrence time of the inflection point is mainly related to the magnitude of  $\text{NO}_2$  decline. In  
173 France,  $\text{NO}_2$  declined less (27.1%), and the time for the total number of confirmed new cases to

174 reach an inflection point was delayed. In Germany, the NO<sub>2</sub> emissions decreased the most, by  
175 54.7%, and the total number of confirmed new cases reached an inflection point within 8 days  
176 after lockdown, which occurred earlier than in other countries. For Iran and Switzerland, due to  
177 the relatively low number of confirmed cases, with the decline of NO<sub>2</sub> after the strict control,  
178 confirmed new cases also reached the inflection point earlier. In the the worst-affected states,  
179 United States, NO<sub>2</sub> emissions decreased by an average of 43.1% in New York, Washington and  
180 California, and the total confirmed new cases dropped significantly, showing signs of easing.

181

182 3.5. The results after epidemic control in the COVID-19-hit areas globally.

183 Following the implementation of strict epidemic control measures, the newly confirmed  
184 cases dropped by more than 50% within 30 days and NO<sub>2</sub> declined significantly in most  
185 countries (Figure 5a). Especially in most countries in Europe and the Western Pacific region, the  
186 number of newly confirmed cases dropped more markedly, with an average drop of more than  
187 60%. The newly confirmed cases in Ireland, Austria, Japan fell by more than 80%. The reduction  
188 in the number of newly confirmed cases is closely related to the intensity of interventions, and  
189 NO<sub>2</sub> can quantify the effects and intensity of interventions. Among the top 50 countries with the  
190 cumulative number of confirmed cases, the stricter the control measures, the higher the rate of  
191 decrease in newly confirmed cases (Figure 5b). If the NO<sub>2</sub> reduction rate is only about 25%, the  
192 control effect of government intervention measures on the epidemic situation is not significant  
193 (Figure 5b).

194 In Germany, when large public events were canceled, the spreading rate ( $\lambda$ ) dropped from  
195 0.43 to 0.25. When schools, childcare facilities, and many stores were closed,  $\lambda$  dropped to 0.15.  
196 Only when a contact ban was imposed by government authorities,  $\lambda$  dropped to 0.09, which is  
197 lower than the recovery speed, and the exponential growth of new cases turned to decline  
198 (Dehning et al., 2020). In Wuhan, China, due to the strict lockdown, the estimated effective  
199 reproduction number  $R_t$  fell immediately after reaching a peak of 3.82 on January 24 and fell  
200 below 1.0 on February 6, 2020 ( $\text{NO}_2$  mutation time) (Pan et al., 2020). In summary, stringent  
201 interventions help to reduce newly confirmed cases earlier and more rapidly.  $\text{NO}_2$  can be used as  
202 an environmental indicator for quantitative research to assess the efficacy and timing of  
203 non-pharmacological interventions to guide current and future responses to global pandemics.

204

## 205 **4. Discussion**

206 Urbanization and rapid transportation system development accelerate the spread of  
207 COVID-19, and only strict containment measures can effectively prevent a second and third  
208 outbreak (Huang et al., 2020b; Huang et al, 2020c). The  $\text{NO}_2$  concentration can be considered an  
209 inexpensive indicator of virus transmission control. As a result of strict control measures and the  
210 rapid implementation of first-level emergency measures, the  $\text{NO}_2$  emissions and total number  
211 confirmed new cases significantly decreased in China, especially in the strictly controlled cities.  
212 In many European countries, a strict lockdown is also effective and easy to do to prevent the  
213 spread of the virus. But there are also areas such as southern and northern Spain and parts of the  
214 United States where the  $\text{NO}_2$  level has increased.

215 Studies have shown that the likelihood of fewer cases in the gradual multi-stage policy is  
216 zero, and that such a policy decision implies that the government is willing to risk an increase in  
217 COVID19 cases and deaths in exchange for decreased economic and isolation impacts, which  
218 may not be desirable from an objective point of view (Karnon, 2020). Although the immediate  
219 adoption of a lockdown policy may lead to many people being adversely affected financially, in  
220 the short term, the number of new confirmed cases will decline approximately 15 days after  
221 policy implementation, and an earlier decline can occur with stricter lockdown measures.  
222 International guidance supports a range of mandatory social isolation measures, extensive case  
223 detection, and isolation and contact tracing. Compliance with quarantine directives is absolutely  
224 critical to saving lives, protecting the most vulnerable in society, and ensuring that the national  
225 security system can cope and care for the sick (Iacobucci, 2020). In such cases, an immediate  
226 lockdown policy may be preferred, and NO<sub>2</sub>, as an environmental indicator of virus control, can  
227 help managers implement effective control measured to curb the spread of COVID-19. In  
228 addition, NO<sub>2</sub> evolution can be used to predict the COVID-19 newly confirmed cases, using the  
229 local NO<sub>2</sub> change rate to reflect the effects of the control measures of governments in various  
230 countries. For details, please refer to the Global Prediction System of the COVID-19 Pandemic  
231 (<http://covid-19.lzu.edu.cn>).

232

## 233 **5. Conclusion**

234 By combining historical COVID-19 data, NO<sub>2</sub> satellite data and government control  
235 measures, we analyzed the quantification and control effects of epidemic intervention measures.  
236 The inflection point and reduction rate of newly confirmed cases are closely related to the time

237 and intensity of epidemic control measures. The decline rate of NO<sub>2</sub> is influenced by the  
238 emission characteristics of each country, on the other hand, it is largely related to the intensity  
239 and implementation effect of control measures. Therefore, NO<sub>2</sub> can be used as an environmental  
240 indicator to quantify the effectiveness and intensity of interventions and can be incorporated into  
241 assessments of the implementation of existing outbreak control measures in countries and into  
242 prediction of future scenarios and case numbers. In addition, NO<sub>2</sub> would help provide  
243 policymakers with information on strengthening, easing and selecting appropriate measures to  
244 contain COVID-19 and other future global pandemics.

245

## 246 Reference

- 247 Baccini L, Brodeur A. Explaining governors' response to the COVID-19 pandemic in the United  
248 States. 2020.
- 249 Bauwens M, Compernelle S, Stavrakou T, Müller JF, Van Gent J, Eskes H, Levelt PF, Vander  
250 R, Veeffkind JP, Vlietinck J, Yu H, Zehner C. Impact of coronavirus outbreak on NO<sub>2</sub>  
251 pollution assessed using TROPOMI and OMI observations. *Geophys Res Lett* 2020; 47.
- 252 Brnnum-Hansen H, Bender AM, Andersen ZJ, Sørensen J, Bønløkke JH, Boshuizen H, Becker T,  
253 Diderichsen F, Loft S. Assessment of impact of traffic-related air pollution on morbidity  
254 and mortality in Copenhagen Municipality and the health gain of reduced exposure.  
255 *Environ Int* 2018; 121: 973-980.
- 256 Chen Y, Liu Q, Geng F, Zhang H, Cai C, Xu T, Ma X, Li H. Vertical distribution of optical and  
257 micro-physical properties of ambient aerosols during dry haze periods in Shanghai.  
258 *Atmos Environ* 2012; 50: 50-59.
- 259 Clougherty JE, Kheirbek I, Eisl HM, Ross Z, Pezeshki G, Gorczynski JE, Johnson S, Markowitz  
260 S, Kass D, Matte T. Intra-urban spatial variability in wintertime street-level  
261 concentrations of multiple combustion-related air pollutants: The New York City  
262 Community Air Survey (NYCCAS). *J Expo Sci Env Epid* 2013; 23: 232-240.
- 263 Curier RL, Kranenburg R, Segers AJS, Timmermans RMA, Schaap M. Synergistic use of OMI  
264 NO<sub>2</sub> tropospheric columns and LOTOS-EUROS to evaluate the NO<sub>x</sub> emission trends  
265 across Europe. *Remote Sens of Environ* 2014; 149: 58-69.
- 266 Dehning J, Zierenberg J, Spitzner FP, Wibral M, Neto JP, Wilczek M, Priesemann V. Inferring  
267 change points in the spread of COVID-19 reveals the effectiveness of interventions.  
268 *Science* 2020.
- 269 Fan X, Dawson J, Chen M, Qiu C, Khalizov A. Thermal stability of particle-phase  
270 monoethanolamine salts. *Environ Sci Tech* 2018; 52: 2409-2417.
- 271 EEA. Air pollution goes down as Europe takes hard measures to combat coronavirus. 2020.
- 272 Flaxman S, Mishra S, Gandy A. Estimating the number of infections and the impact of  
273 nonpharmaceutical interventions on COVID-19 in 11 European countries. Imperial  
274 College COVID-19 Response Team 2020.

- 275 Han KM. Temporal Analysis of OMI-Observed Tropospheric NO<sub>2</sub> Columns over East Asia  
276 during 2006-2015. *Atmos* 2019; 10: 658.
- 277 Huang C, Wang Y, Li X, Ren L, Zhao J, Hu Y, Zhang L, Fan G, Xu J, Gu X, Cheng Z, Yu T,  
278 Xia J, Wei Y, Wu W, Xie X, Yin W, Li H, Liu M, Xiao Y, Gao H, Guo L, Xie J, Wang G,  
279 Jiang R, Gao Z, Jin Q, Wang J, Cao B. Clinical features of patients infected with 2019  
280 novel coronavirus in Wuhan, China. *Lancet* (London, England) 2020a.
- 281 Huang F, Zhou J, Chen N, Li Y, Wu S. Chemical characteristics and source apportionment of  
282 PM<sub>2.5</sub> in Wuhan, China. *J Atmos Chem* 2019; 76: 245-262.
- 283 Huang J, Liu X, Zhang Li, Yang K, Chen Y, Huang Z, Liu C, Lian X, Wang D. The amplified  
284 second outbreaks of global COVID-19 pandemic. *medRxiv* 2020b.
- 285 Huang Q, Cheng S, Perozzi RE. Use of a MM5-CAMx-PSAT Modeling System to Study SO<sub>2</sub>  
286 Source Apportionment in the Beijing Metropolitan Region. *Environ Model Assess* 2012;  
287 17: 527-538.
- 288 Huang Z, Huang J, Gu Q, Du P, Liang H, Dong Q. Optimal temperature zone for the dispersal of  
289 COVID-19. *Sci Total Environ* 2020c: 139487.
- 290 Iacobucci G. Covid-19: UK lockdown is "crucial" to saving lives, say doctors and scientists.  
291 *Bmj-Brit Med J* 2020; 368.
- 292 Johansson C, Lovenheim B, Schantz P, Wahlgren L, Almstrom P, Markstedt A, Stromgren M,  
293 Forsberg B, Sommar J. Impacts on air pollution and health by changing commuting from  
294 car to bicycle. *Sci Total Environ* 2017; 584: 55-63.
- 295 Karnon J. A Simple Decision Analysis of a Mandatory Lockdown Response to the COVID-19  
296 Pandemic. *Appl health econ hea* 2020; 18: 329-331.
- 297 Khalil MAK, Rasmussen, R. A. Carbon Monoxide in an Urban Environment: Application of a  
298 Receptor Model for Source Apportionment. *Japca* 1988; 38: 901-906.
- 299 Kim Y, Guldman JM. Land-use regression panel models of NO<sub>2</sub> concentrations in Seoul, Korea.  
300 *Atmos Environ* 2015; 107: 364-373.
- 301 Legido-Quigley H, Mateos-Garcia JT, Campos VR, Gea-Sanchez M, Muntaner C, McKee M.  
302 The resilience of the Spanish health system against the COVID-19 pandemic. *Lancet*  
303 *Public heal* 2020; 5: e251-e252.

- 304 Li Q, Guan X, Wu P, Wang X, Zhou L, Tong Y, Ren R, Kathy SML, Eric HYL, Jessica YW,  
305 Xing X, Xiang N. Early Transmission Dynamics in Wuhan, China, of Novel Coronavirus  
306 –Infected Pneumonia. *New Engl J Med* 2020.
- 307 Lian X, Huang J, Huang R, Liu C, Wang L, Zhang T. Impact of city lockdown on the air quality  
308 of COVID-19-hit of Wuhan city. *Sci Total Environ* 2020: 140556.
- 309 Liu D, Deng Q, Ren Z, Zhou Z, Song Z, Huang J, Hu R. Variation trends and principal  
310 component analysis of nitrogen oxide emissions from motor vehicles in Wuhan City from  
311 2012 to 2017. *Sci Total Environ* 2020; 704: 134987.
- 312 Pan A, Liu L, Wang C, Guo H, Hao X, Wang Q, Huang J, He N, Yu H, Lin X. Association of  
313 public health interventions with the epidemiology of the COVID-19 outbreak in Wuhan,  
314 China. *JAMA* 2020; 323: 1915-1923.
- 315 Paterlini M. Lockdown in Italy: personal stories of doing science during the COVID-19  
316 quarantine. *Nature* 2020.
- 317 Schiermeier Q. Why pollution is plummeting in some cities - but not others. *Nature* 2020; 580:  
318 313.
- 319 Cyranoski D, Silver A. Wuhan scientists: What it's like to be on lockdown. *Nature* 2020.
- 320 Tessum MW, Larson T, Gould TR, Simpson CD, Yost MG, Vedal S. Mobile and Fixed-Site  
321 Measurements To Identify Spatial Distributions of Traffic-Related Pollution Sources in  
322 Los Angeles. *Environ Sci Tech* 2018; 52: 2844-2853.
- 323 Tian H, Liu Y, Li Y, Wu C, Chen B, Kraemer MUG, Li B, Cai J, Xu B, Yang Q. An  
324 investigation of transmission control measures during the first 50 days of the COVID-19  
325 epidemic in China. *Science* 2020; 368: 638-642.
- 326 Wei Y, Wei L, Jiang Y, Shen S, Zhao Y, Hao Y, Du Z, Tang J, Zhang Z, Jiang Q.  
327 Implementation of Clinical Diagnostic Criteria and Universal Symptom Survey  
328 Contributed to Lower Magnitude and Faster Resolution of the COVID-19 Epidemic in  
329 Wuhan. *Engineering* 2020.
- 330 Wu JT, Leung K, Leung GM. Nowcasting and forecasting the potential domestic and  
331 international spread of the 2019-nCoV outbreak originating in Wuhan, China: a  
332 modelling study. *Lancet (London, England)* 2020.
- 333 Yuan B, Hu W, Shao M, Wang M, Chen W, Lu S, Zeng L, Hu M. VOC emissions, evolutions  
334 and contributions to SOA formation at a receptor site in eastern China. *Atmos Chem*  
335 *Phys* 2013; 13: 8815-8832.

336 Zhou Z, Tan Q, Liu H, Deng Y, Wu K, Liu C, Zhou X. Emission characteristics and  
337 high-resolution spatial and temporal distribution of pollutants from motor vehicles in  
338 Chengdu, China. Atmos Pollut Res 2019; 10: 749-75.

339 **Corresponding Author**

340 Dr. Jianping Huang ( [hjp@lzu.edu.cn](mailto:hjp@lzu.edu.cn) )

341

342 **Acknowledgements**

343 This work was jointly supported by the National Science Foundation of China (41521004)  
344 and the Gansu Provincial Special Fund Project for Guiding Scientific and Technological  
345 Innovation and Development (Grant No. 2019ZX-06). The authors acknowledge the China  
346 National Environmental Monitoring Centre for providing the datasets. <http://www.cnemc.cn/>.

347

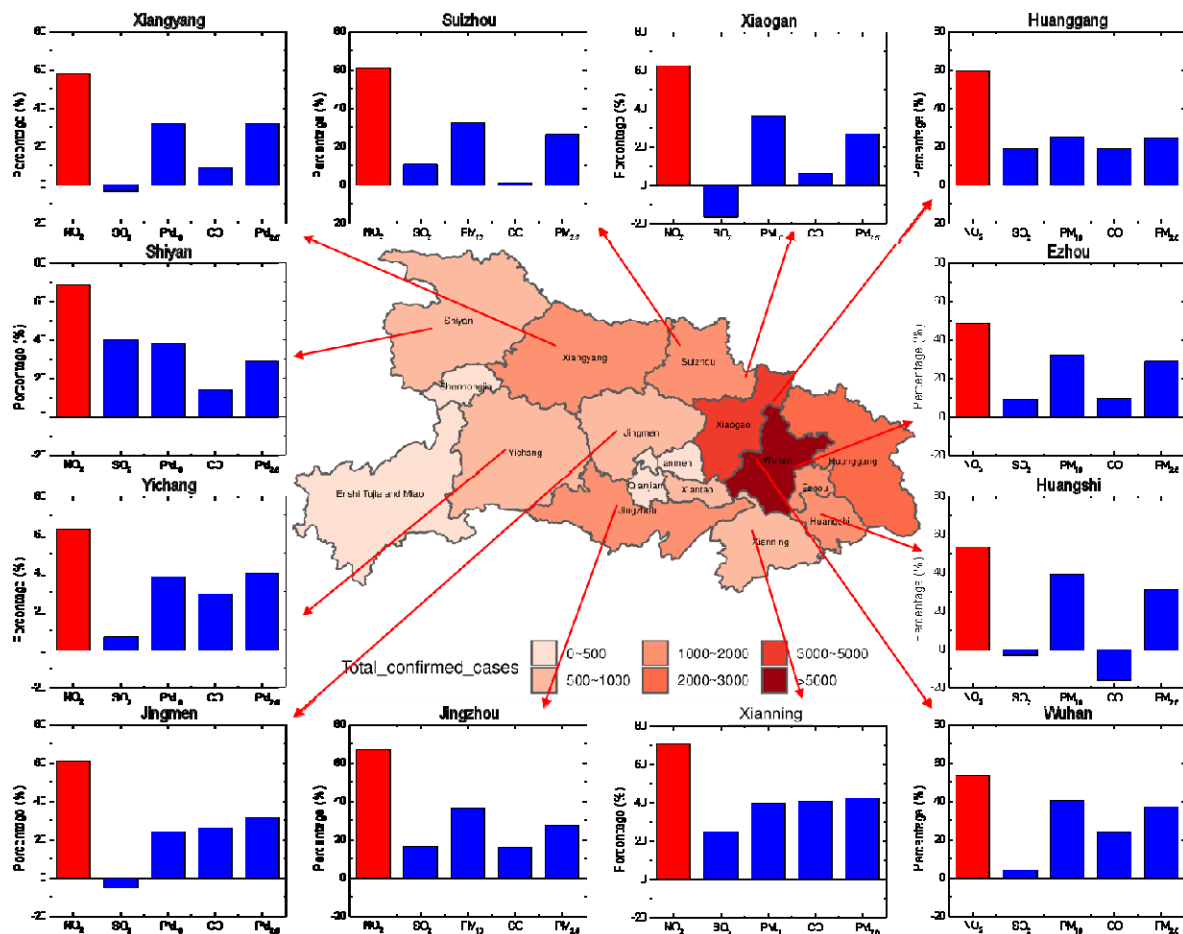
348 Additional information

349 Competing financial interests: The authors declare no competing financial interests.

350

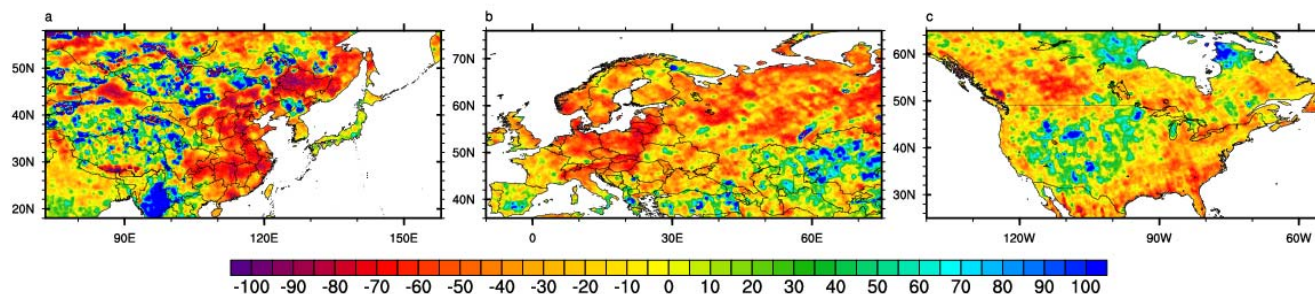
351 Graphics software

352 All maps and plots were produced using licensed.



353

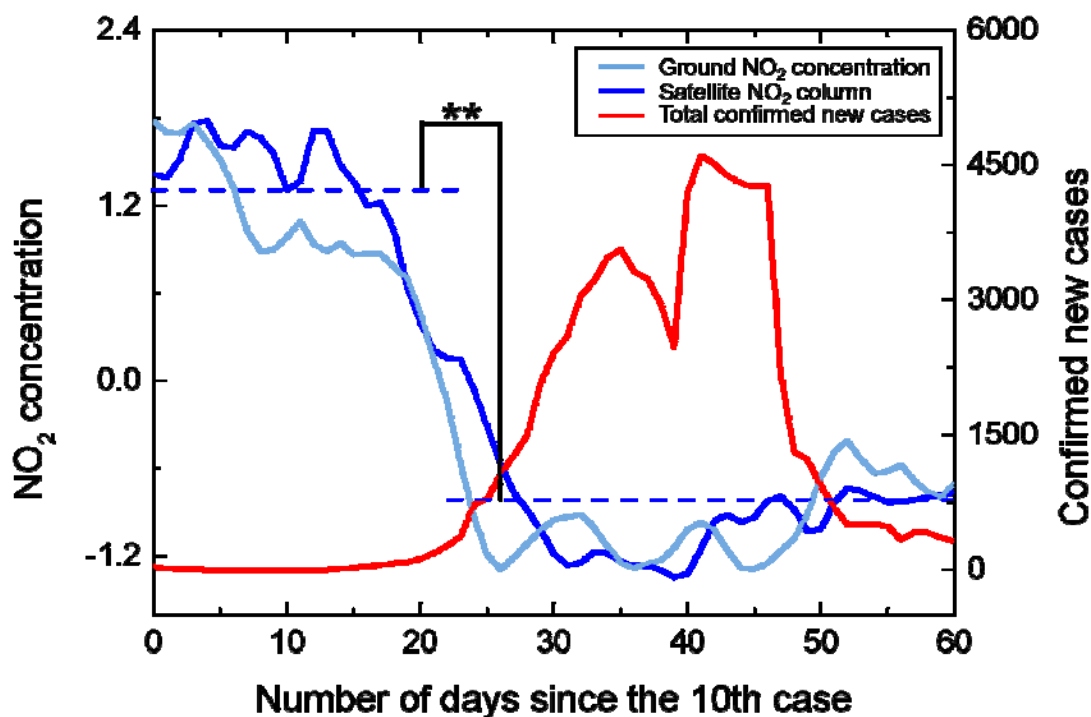
354 **Fig. 1** The improvement rate of the major pollutants and the distribution of the  
 355 **accumulated epidemic numbers in each city of Hubei Province after the lockdown.** One  
 356 month after the blockade (23 February 2020), the cumulative number of confirmed cases ranged  
 357 from 0-46607 (Wuhan), as indicated by the colour scale. The monthly mean improvement rate of  
 358 NO<sub>2</sub>, SO<sub>2</sub>, PM<sub>10</sub>, CO and PM<sub>2.5</sub> after the lockdown in the worst virus-affected areas is shown in  
 359 the histogram, with SO<sub>2</sub>, PM<sub>10</sub>, CO and PM<sub>2.5</sub> indicated with blue columns, and NO<sub>2</sub> indicated  
 360 with red columns. Red columns (NO<sub>2</sub>) are significantly higher than the others, so it can  
 361 characterize the locking measures.



362

363 **Fig. 2 The relative variation in the monthly average tropospheric NO<sub>2</sub> concentration before**  
364 **and after the lockdown. a, Relative variation in East Asia. b, Relative variation in Western**  
365 **Europe. c, Relative variation in North America. The colour table represents the relative**  
366 **percentage of the monthly average change in NO<sub>2</sub> after the lockdown compared to the before.**  
367 **The red areas indicate that the NO<sub>2</sub> concentration decreased, and the blue areas indicate that the**  
368 **NO<sub>2</sub> concentration increased. The lockdown in East Asia, Western Europe and North America**  
369 **began on January 23, March 10, and March 16, respectively. Source: Analysis of data from the**  
370 **NASA Ozone Monitoring Instrument (OMI).**

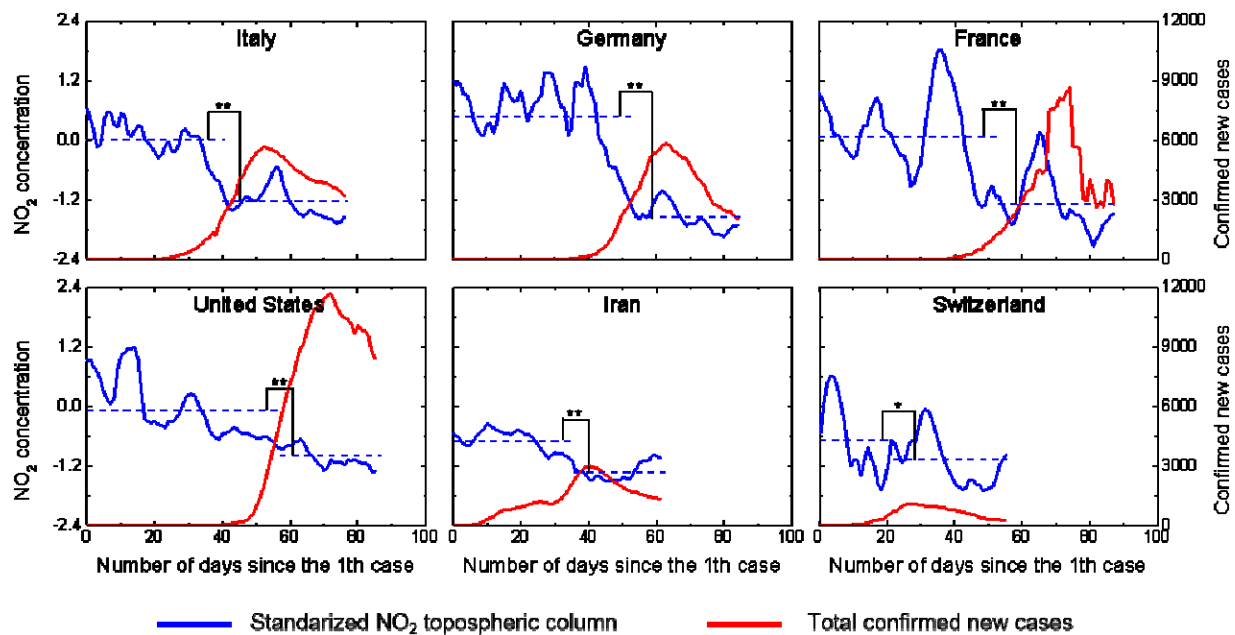
371



372

373 **Fig. 3** Temporal variation in the NO<sub>2</sub> concentration and number of new cases in China. The  
374 standardized 7-day smooth data of NO<sub>2</sub> is represented by blue lines, with satellite observations in  
375 dark blue and ground observations in light blue. The dotted line indicates the average value of  
376 NO<sub>2</sub> before and after the blockade. The 7-day smooth data of total confirmed new cases is  
377 indicated by red lines. \*\* indicates significant difference at the 0.01 level (bilateral), and \*  
378 indicates significant difference at the 0.05 level (bilateral). Starting from the lockdown, the NO<sub>2</sub>  
379 concentration dropped significantly, and the number of new cases also showed a downward trend  
380 within two weeks.

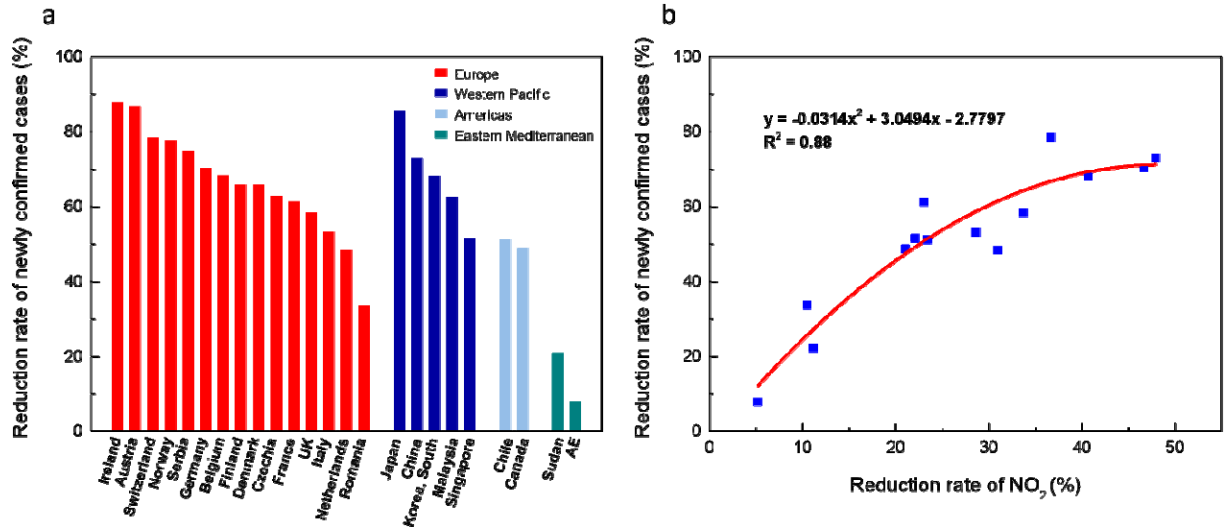
381



382

383 **Fig. 4** Temporal variation in the NO<sub>2</sub> concentration and number of new cases in the  
384 COVID-19-hit areas. Italy, Germany, France, the United States, Iran and Switzerland were  
385 selected as the representatives of COVID-19-hit areas. New York, Washington and California  
386 were selected as the representatives of the United States. From the time of the first case in each  
387 country to 20 April 2020, the standardized 7-day smooth satellite data of NO<sub>2</sub> is represented by  
388 the blue line. The dotted line indicates the average value of NO<sub>2</sub> before and after the blockade.  
389 The 7-day smooth data of total confirmed new cases is indicated by red line. \*\* indicates  
390 significant difference at the 0.01 level (bilateral), and \* indicates significant difference at the  
391 0.05 level (bilateral). The NO<sub>2</sub> in major countries showed a downward trend. The total confirmed  
392 new cases decreased significantly about 15 days after the lockdown.

393



394

395 **Fig 5. The results of strict epidemic control measures.** a, The reduction rate of new  
396 confirmed cases within 30 days at the NO<sub>2</sub> mutation point. Red represents Europe, dark blue  
397 represents Western Pacific, light blue represents Americas, and green represents Eastern  
398 Mediterranean. b, Changes in the rate of decline in NO<sub>2</sub> and the reduction rate of newly  
399 confirmed cases after the implementation of strict epidemic control measures.